TSR The Sedimentary Record
SEPM | Society for Sedimentary Geology

Cunningham, C. M., & Arnott, R. W. C. (2023). Outsized Turbidity Currents as a Primary Mechanism for Neoproterozoic Organic Carbon Delivery to the Deep Sea. *The Sedimentary Record*, *21*(2). https://doi.org/10.2110/001c.77519

Research Article

Outsized Turbidity Currents as a Primary Mechanism for Neoproterozoic Organic Carbon Delivery to the Deep Sea

Celeste M. Cunningham[1,2], R. William C. Arnott[2]

[1] Earth Sciences, St. Francis Xavier University, [2] Earth and Environmental Science, University of Ottawa

Keywords: organic carbon, turbidites, Neoproterozoic, deep marine levees

https://doi.org/10.2110/001c.77519

The Sedimentary Record
Vol. 21, Issue 2, 2023

Levees in modern deep-marine systems have been shown to sequester significant amounts of organic carbon due largely to their expanse and high rates of sedimentation. However, relatively few studies have examined organic carbon sequestration in ancient deep-marine leveed slope channel systems. Physical and geochemical analyses of well-exposed levee deposits in the Neoproterozoic Windermere Supergroup in B.C., Canada have shown that intervals of organic-rich (up to 4% TOC) strata correlate with conditions of elevated sea level and primary productivity on the shelf. Organic matter (OM) occurs primarily as micro- to nano-scale carbon adsorbed onto the surface of clay grains and notably occurs mostly in anomalously thick, mud-rich sandstone beds that are interspersed within successions of thin-bedded, comparatively organic-poor turbidites. The concentration of organic carbon in thick beds suggests that even when primary productivity is high it only becomes mobilized in significant quantities into the deep sea by uncommon, outsized turbidity currents. Although markedly more common in organic-rich intervals, thick, organic-rich beds occur also in organic-poor levee deposits, suggesting that the occurrence and frequency of outsized flows may be linked to primary productivity on the shelf. High rates of OM production and fallout would result in rapid accumulation of OM on the seafloor that then binds and provides mechanical strength to the accumulating sediment. Later this overthickened, organic-rich sediment pile becomes gravitationally unstable and ultimately remobilized downslope. These failure events create large, surge-like flows that are considerably thicker than the depth of the slope channels through which they travel. Accordingly, continuous overspill over the channel margins results in the deposition of an anomalously thick, sand- and organic-rich bed. These episodic events not only deplete the outer continental shelf of OM, but apparently also reduces the gradient slope of the local seabed, which then results in the more typical smaller, channel-confined organic-poor turbidity currents. Additionally, the abrupt and single-bed occurrence of OM-rich strata suggests that the buildup of organic-rich strata and seafloor stabilization was rapid but only of limited duration.
Significantly, this study suggests that outsized turbidity currents that originate on the outer continental shelf are the primary mechanism for organic matter delivery to the deep sea, at least in pre-vegetation times, and that flow size and frequency, in addition to primary productivity, exerts an important control on the distribution of organic carbon in deep-sea sediments.

INTRODUCTION

Deep-sea fan systems are significant reservoirs of buried organic carbon, making them an important part of the global carbon cycle (e.g., Baudin et al., 2010; Cunningham & Arnott, 2023; Galy et al., 2007; Hage et al., 2022; Hussain et al., 2021; Masiello, 2007).

Organic carbon has been reported from a range of deep-marine sedimentary environments, including basin-floor lobes and slope channels and levees (Baudin et al., 2010, 2017, 2020; Cunningham et al., 2023; Cunningham & Arnott, 2023; Hussain et al., 2021; McArthur et al., 2017; McArthur, Kneller, Souza, et al., 2016; McArthur, Kneller, Wakefield, et al., 2016; Saller et al., 2006; Stetten et al., 2015), and that turbidity currents have been shown to be effective mechanisms for its transport from shallow continental margins to more distal parts of the depositional system (e.g., Saller et al., 2006; de Baudin et al., 2010, 2017, 2020; Cunningham & Arnott, 2023; Galy et al., 2007; Hage et al., 2020, 2022; Hussain et al., 2021; Lee et al., 2019; Masiello, 2007; Stetten et al., 2015). Studying the occurrence and stratigraphic distribution of organic-rich strata can provide insight into the physical processes that govern the transport and deposition of organic matter to the deep ocean and source-to-sink trends from the continental realm to the deep marine.

Recent work on Neoproterozoic slope deposits in Western Canada has shown that organic carbon occurs mostly in thick-bedded sandstones in levee deposits (Cunningham et al., 2023; Cunningham & Arnott, 2023). Although the physical and chemical processes that occur during the deposition of a these organic-rich beds have previously been described in detail by Cunningham and Arnott (2023) and shown to be related to various external environmental factors, such as primary productivity, sea level, weathering, and sediment flux (Cunningham et al., 2023), the characteristics of the organic-rich flows themselves have received much less attention. Here, we present descriptions of the stacking patterns of organic-rich beds from this site and discuss the size and frequency of flows that transport organic matter to the deep-marine, in addition to their possible triggering mechanisms. Importantly, these results help to identify basin-scale factors that control the distribution of organic carbon in deep-sea sediments.

GEOLOGICAL SETTING

The study area is located in the Cariboo Mountains of east-central British Columbia, Canada (Figure 1) where strata of the Neoproterozoic Windermere Supergroup crop out extensively and record the breakup of Rodinia and subsequent sedimentation along a passive continental margin. The base of the succession consists of intercalated glacial diamictites and mafic volcanics related to early rifting (Eyster et al., 2018). This is overlain by a post-rift succession of deep-water (Kaza Group and Isaac Formation) to shallow shelf and platform sedimentary rocks (Cunningham and Yankee Belle formations) (Campbell et al., 1973) that record the progradation of the passive continental margin into the thermally subsiding proto-Pacific Ocean (Figure 2) (Ross, 1991; Ross et al., 1995; Ross & Arnott, 2007).

Age control of the Windermere Supergroup in this area is generally poor due to a paucity of datable markers and absence of biostratigraphy; age being largely constrained by radiometric dates from below (736 – 728 Ma; Evenchick et al., 1984; Eyster et al., 2018; McDonough & Parrish, 1991) and above (570 +/- 5.3 Ma; Colpron et al., 2002) its bounding unconformities. Within the Windermere succession dates are limited to a maximum depositional age of 650 Ma based on U-Pb dating of detrital zircons (Hadlari et al., 2021), and a Re-Os isochron date of 607.8 +/- 4.7 Ma from organic-rich mudstones of the Old Fort Point Formation (Kendall et al., 2004; Smith et al., 2014).

Study Area

The Castle Creek study area is located on a vertically dipping limb of a southwest-verging anticline. Strata are recently deglaciated, vegetation-free, and superbly exposed in a section approximately 2.6 km thick and up to 8 km wide (Navarro & Arnott, 2020; Terlaky et al., 2015). Basin-floor deposits of the upper Kaza Group make up the lower ~800 m of the exposed succession and are overlain by ~1.8 km of slope deposits of the Isaac Formation (Figure 2). The Isaac Formation comprises at least seven up to 200 m-thick, coarse-grained, laterally discontinuous sandstone and conglomerate units, surrounded by thin-bedded, mudstone-rich strata. These discontinuous sandstones and conglomerates are interpreted to be the fill of slope-channel complexes bounded by finer-grained, genetically related levees (Figure 3), and are informally termed Isaac Channel Complex 0 – 6 (ICC0 – ICC6). The levee deposits of ICC3 and ICC4 are particularly well-developed, and their sedimentology, stratigraphic architecture, and geochemistry have been described in detail by Khan and Arnott (2011), Khan et al. (2011), Cunningham and Arnott (2021, 2023); Bergen et al. (2022), and Cunningham et al. (2023). Notably, although organic-rich strata are generally uncommon in the study area, organic-rich beds are abundant in a 60-m-thick interval in levee deposits below ICC4 (Cunningham et al., 2023; Cunningham & Arnott, 2023).

METHODS

Levee deposits at the Castle Creek study site were logged in bed-by-bed detail to capture trends in lithology, stratal thickness, sedimentary structures, and grain size. This was combined with geochemical analyses, principally total organic carbon (TOC) (Cunningham et al., 2023; Cunningham & Arnott, 2023), to identify organic-rich strata and its stratigraphic distribution. In total 340 m of continuous vertical stratigraphy was logged in cm-scale detail (Figure 3). Stratigraphic logs were spaced 40-70 m apart along the strike of the outcrop and individual beds were correlated over ~ 2 km in the field and later combined into a single composite log. Turbidites are described using the five-division terminology of Bouma (1962).

Turbidites rarely contain all five divisions; instead typically comprising only part of the full sequence. *Lower-division* turbidites consist of the bottom two divisions (T_a and T_b), whereas *upper-division* turbidites comprise only the upper two or three divisions (T_c, T_d, and T_e).

RESULTS

Organic-rich strata at the Castle Creek study site are primarily confined to one 60-meter-thick stratigraphic interval in levee deposits immediately below ICC4, which previously was reported to correlate with conditions of elevated sea level and primary productivity on the continental shelf (Figure 4) (Cunningham et al., 2023; Cunningham & Arnott, 2023). Organic-rich beds account for ~5% of the measured stratigraphy in this study and are divided into two facies: organic-rich mudstone and organic-rich sandstone turbidites. TOC in these organic-rich facies ranges from 0.4 – 4.04 % (Cunningham & Arnott, 2023), which if corrected for lower greenschist metamorphism (and the loss of ~50-80% of the original organic content) may be of the order of 2 –16% (Hayes et al., 1983; Smith et al., 2014; Tissot & Welte, 1978). Organic-rich sandstone turbidites account for ~ 85% of the organic-rich strata at this site. The sedimentology and geochemistry of these facies are summarized below; for detailed descriptions see in Cunningham and Arnott (2023).

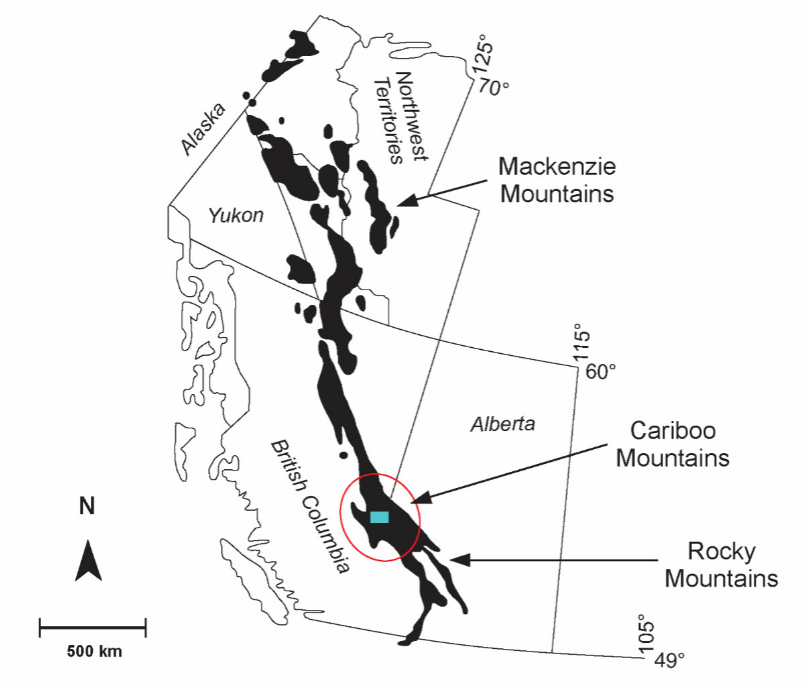

Figure 1. A) Distribution of exposed Windermere Supergroup stratigraphy (black polygons) in western Canada. Deep-marine rocks are especially well exposed in the Cariboo Mountains (red circle) and at the Castle Creek study area (blue box).

Levee deposits at the Castle Creek study site are dominated by very thin- to thin-bedded (1 – 15 cm), upper-division turbidites (~72% of turbidites in the measured section) (Bergen et al., 2022; Cunningham & Arnott, 2021; Z. A. Khan & Arnott, 2011). Interspersed with these levee thin beds are uncommon, organic-poor, medium- to thick-bedded (generally 20 – 80 cm thick), lower-division turbidites and organic-rich sandstone turbidites. These latter strata range from 30 – 140 cm thick and are distinctively banded, with alternating layers of orange, highly dolomite-cemented sandstone, and black, mud-rich sandstone (Figure 4). Most of the organic matter in these beds occurs in the black bands as micro- to nano-scale coatings on clay particles, although uncommon sand-sized amorphous grains and organo-mineralic aggregates are also present in the cemented orange bands. The unique banding in these beds (informally termed "tiger-striped" beds) is interpreted to result from alternating periods of turbulent and cohesive flow conditions as organic-rich turbidity currents overspilled channel margins and deposited on the levee (Cunningham & Arnott, 2023). The high cement content (up to 35%) in the orange bands, which consists of ferroan dolomite, is interpreted to have formed from processes related to the diagenesis of the organic matter (Boles, 1978; Cunningham & Arnott, 2023; Curtis, 1978; Kelts & McKenzie, 1982; Mazzullo, 2000).

Organic-rich sandstone turbidites occur as single beds that are separated by 2 – 22 m in a thick succession of comparatively organic-poor (< 0.4% TOC) thin-bedded turbidites. These beds are laterally continuous over distances of several hundreds of meters and show only a slight thinning away from the channel. Although sand-rich tiger-striped beds occur exclusively in the single 60-m-thick interval below ICC4, rare organic-rich mudstone beds crop out elsewhere in the 340-m thick succession (Cunningham et al., 2023). Deformed organic-rich mudstones have also been observed in mass transport deposits (slides and debrites) at Castle Creek, which notably also contain fragments of oolitic and stromatolitic limestone (Bergen et al., 2022).

DISCUSSION

The concentration of organic matter in anomalously thick, sand-rich turbidites provides important information about both the source and depositional history of these beds. Previous work on levee deposits, both at Castle Creek and elsewhere, has shown that thick, coarse-grained, lower-division turbidites are generally the result of large, sand-rich turbidity currents whose thickness is significantly greater than the height of the channel, resulting in continuous overspill of coarse-grained sediment onto the levee, or as part of overbank splay deposits (Arnott, 2010; Cunningham & Arnott, 2021; Kane et al., 2007; Peakall et al., 2000; 2023). This contrasts with the conditions for thin-bedded levee turbidites, where the lower, coarser-grained portion of the flow remains mostly confined in the channel and only lesser amounts of fine-grained sediment from the upper, dilute portion of the flow overspill onto the levee (e.g., Bergen et al., 2022). Since most of the organic carbon at the Castle Creek study area occurs in unusually thick, sand-rich turbidites, this suggests that organic matter was primarily delivered to the deep marine by anomalously large, coarse-grained turbidity currents, which were of sufficient

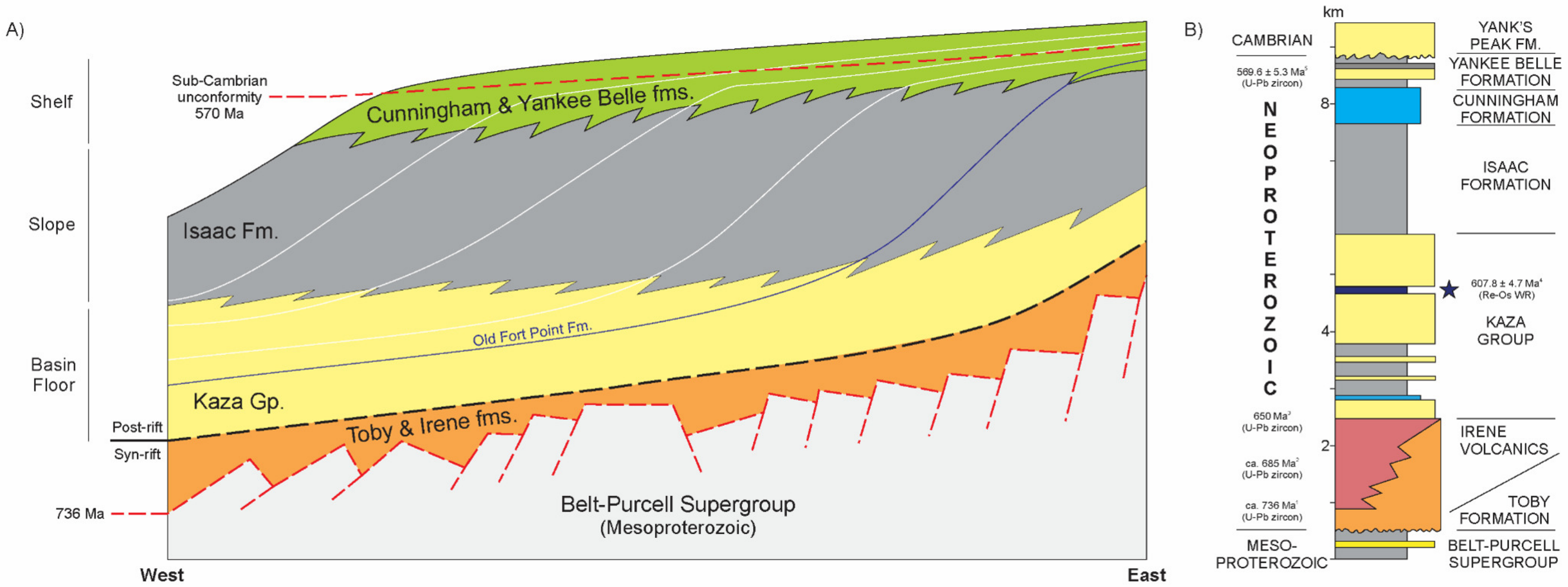

Figure 2. A) Schematic of Windermere Supergroup stratigraphy in the Cariboo Mountains, east-central British Columbia showing progradation of the continental margin system toward the west (modified from Hadlari et al., 2021). B) General stratigraphic column of the Windermere Supergroup in the Cariboo Mountains (Z. Khan, 2012). Radiometric ages are from 1McDonough and Parrish (1991), 2Lund et al. (2003), 3Hadlari et al. (2021), 4Kendall et al. (2004) and 5Colpron et al. (2002).

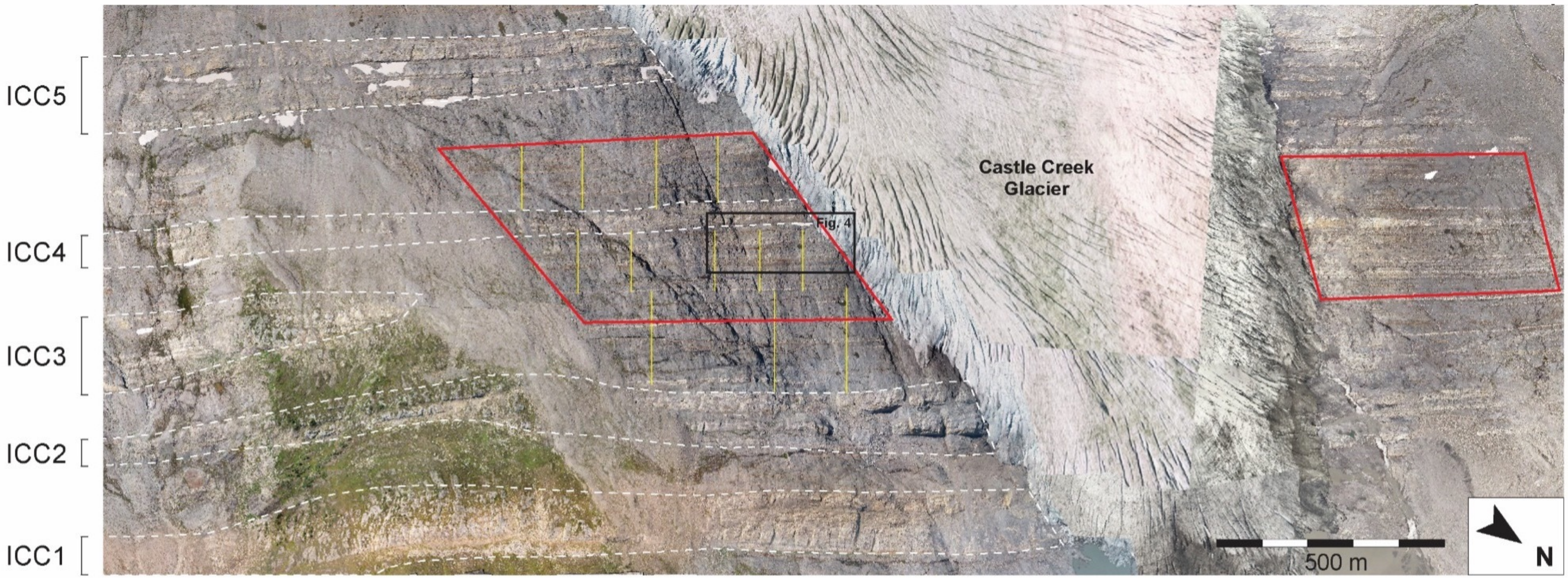

Figure 3. Aerial photomosaic showing slope deposits of the Isaac Formation at Castle Creek, with Isaac Channel Complex Sets 1 – 5 labelled on the left and outlined with white dashed lines (Isaac Channel Complex Sets 0 and 6 are not shown). Levee deposits of ICC3 and ICC4 are outlined with red polygons. The strata shown in Figure 5 is outlined with a black box. Log locations are shown in yellow.

Facies	Lithology and Structure	Bed thickness and basal contacts	Depositional Interpretation	Bouma Division	Representative Photo
Organic-rich sandstone	Planar-stratified orange, cemented sandstone overlain by distinctively alternating bands of black, organic- and clay-rich sandstone and orange, cemented sandstone. Black bands consist of dispersed fine-grained quartz sand with ~ 30 - 60 % clay matrix content. Micro- to nano-scale carbon rims surround clay grains, related to adsorption onto the mineral surface. Orange bands consist of quartz sandstone with 5-35% ferroan dolomite cement. Typically capped by ripple cross-stratified, cemented sandstone. Grain size of sand ranges from very fine to fine. TOC ranges from 0.6 – 4.0%.	Beds range from 30 – 140 cm thick. Basal contacts are sharp and generally planar. Orange and black bands are sharply bounded and range from 0.2 – 30 cm thick with common load and flame structures along their base.	Deposited from turbidity currents with abundant cohesive organic matter and clay. Banding forms because of alternating turbulent and cohesive flow conditions in the near-bed region (clean sandstones are deposited under turbulent conditions; clay and OM aggregation and accumulation near the bed create cohesive conditions and deposit clay-rich sand).	N/A	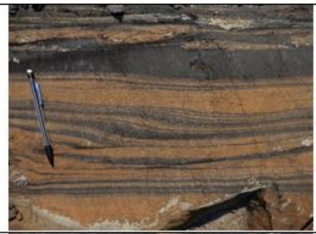
Organic-rich mudstone	Planar thinly laminated black claystone and siltstone. Framboidal pyrite is abundant. TOC ranges from 0.4% to 1.8%.	Beds range from 1 – 8 cm thick. Laminations are < 1 – 4 mm-thick. Basal contacts are sharp and planar.	Deposited by thin, fine-grained, dilute, low-energy turbidity currents.	$T_{d/e}$	
Very thin- to medium-bedded upper division turbidites	Ripple cross-stratified sandstone overlain by thinly laminated siltstone and mudstone. Sandstone is well sorted; grain size ranges from very fine to medium sand.	Bed thickness ranges from < 1 – 28 cm, typically 1 – 15 cm. Basal contacts are usually sharp and planar with common load casts and flame structures.	Deposited from decelerating fine-grained, dilute turbidity currents under moderate (ripple) flow velocities and low rates of suspension fallout.	$T_{c-d/e}$	
Medium- to very thick-bedded lower division turbidites	Graded sandstone with a basal unit of either structureless or planar-stratified sandstone transitioning upwards into ripple cross-stratified sandstone overlain by a thin siltstone or mudstone. Sandstone is moderately to well-sorted and grades upward from coarse- or upper medium-grained sandstone to lower medium- or fine-grained sandstone.	Bed thickness ranges from 14 – 180 cm, but typically 20 – 80 cm. Rare 2 – 5 m-thick amalgamated units. Basal contacts are generally sharp and planar with uncommon scours and mudstone intraclasts.	Deposited by decelerating turbidity currents with grain size ranging from coarse sand to clay. Where present, basal structureless sand (T_a) suggests an initial period of deposition with high rates of suspension fallout followed by more prolonged bed-load transport and lower rates of suspension fallout ($T_{b-d/e}$).	$T_{a-d/e}$	

Table 1. Lithological description and depositional interpretation of facies observed in levee deposits of this study.

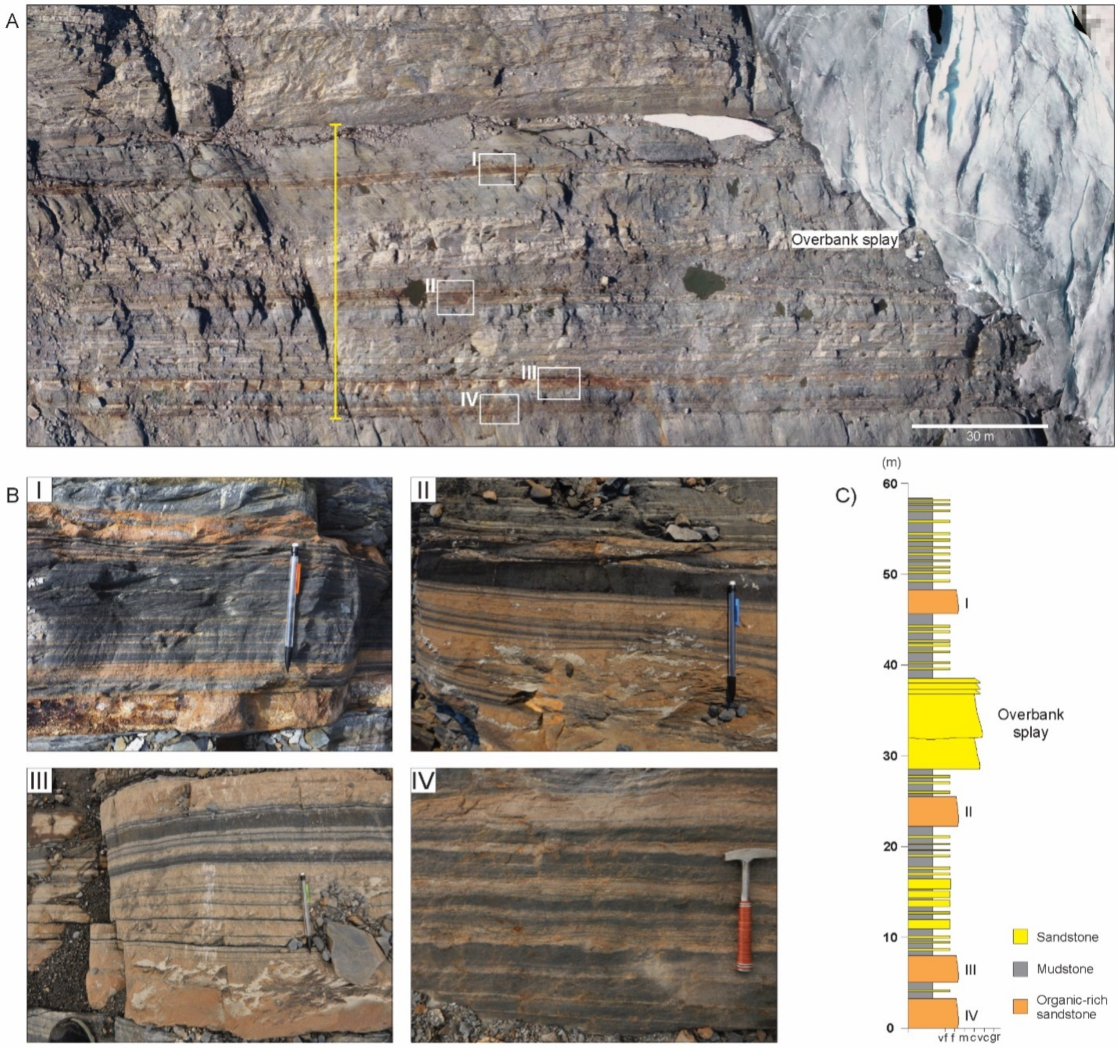

Figure 4. A) Aerial photomosaic of the organic-rich interval below ICC4 (indicated with yellow line). Thick, organic-rich sandstone beds exhibit a distinctive rusty colour. Locations of the photos shown in B and the stratigraphic log in C are highlighted in white. B) Close-up photographs of the four organic-rich beds highlighted in white boxes in A. Note the distinctive orange and black banding within these beds. C) Stratigraphic log detailing the distribution of organic-rich beds among organic-poor levee turbidites.

thickness to continuously overspill the channel margins. Although it is possible that the organic-rich sandstone beds are overbank splay deposits formed when the lower, coarser-grained portion of channelized turbidity currents escape confinement or breach the levee, they differ markedly from other overbank splay deposits at the site, making this unlikely. Splay deposits typically consist of erosionally based, thick-bedded, coarse-grained, structureless and matrix-rich sandstone beds with distinctive along-strike facies changes described in earlier works (e.g., Angus et al., 2019; Bergen et al., 2022; Z. A. Khan & Arnott, 2011; Ningthoujam et al., 2022; Terlaky & Arnott, 2014). Organic-rich sandstone beds contain only fine sand, show only minor erosion at their base, and lack any significant along-strike facies change supporting the interpretation that they derive from the finer-grained, upper part of turbidity currents as they overtopped channel confinement.

Furthermore, because strata are Neoproterozoic in age, the preserved organic matter is exclusively marine and would have originated in warm, shallow waters on the continental shelf and over the upper slope (Behrensmeyer et al., 1992; Butterfield, 2014; Cunningham et al., 2023; Cunningham & Arnott, 2023; Gensel, 2021). The anomalously large flows that mobilized and transported this organic matter downslope would therefore probably also have originated on the shelf rather than the continental slope, where, in contrast, organic matter would be in low abundance or absent. Similarly, interspersed mass-transport deposits with abundant organic matter and scattered oolite and stromatolite fragments are likely to also have originated much higher on the slope, possibly near the shelf-slope break (Bergen et al., 2022). In comparison, the thick-bedded, sand-rich turbidites that are organic-poor are interpreted to reflect periods of low primary productivity on the shelf, or to have originated from slope-derived turbidity currents rather than the shelf.

There are several possible mechanisms for triggering unusually large, shelf-derived flows. For example, earthquakes are known to initiate exceptionally large turbidity currents that flush canyon systems and transport hundreds of cubic kilometers of sediment into the deep sea (e.g., Hsu et al., 2008; Krause et al., 1970; Masson et al., 2011; Mountjoy et al., 2018; Piper & Normark, 2009). Alternatively, recent work monitoring modern continental shelves and canyon systems, such as the Congo River system and the St. Lawrence Estuary, have shown that local shelf conditions can also be conducive to the formation of large flows (e.g., Hage et al., 2019; Normandeau et al., 2020; Talling, 2014; Talling et al., 2022). For example, Talling et al. (2022) recorded the longest runout turbidity currents ever measured in the Congo submarine canyon and linked them to river floods and rapid sediment accumulation at the mouth of the river with later downslope remobilization. However, this is dependent on the deep-water system being linked directly to the river system, for example the modern Congo Canyon and Laurentian Channel. Large storms, especially those with prolonged periods of sustained high winds and wave height (including but not limited to hurricanes and typhoons), have also been linked to large, long-duration turbidity currents (e.g., Normandeau et al., 2020; Porcile et al., 2020; Sequeiros et al., 2019; Zhang et al., 2018). These storms have also been theorized to contribute to river flooding and sediment delivery and accumulation in the river mouth and on the shelf, potentially priming the system for a later downslope transport event. Other potential causes of flooding that could be linked to the triggering of turbidity currents include high seasonal snowmelt or glacial outburst floods (e.g., Bornhold et al., 1994; Russell et al., 2006; Shaw & Gilbert, 1990; Tweed & Russell, 1999; Veh et al., 2019; Weckwerth et al., 2019).

Although all these mechanisms could account for the deposition of thick-bedded, sand-rich levee turbidites, this type of bed is markedly more common in the 60-m-thick organic-rich interval (two thirds of these beds occur here). In this interval, these thick beds are enriched in OM and spaced 2 – 22 m apart. This irregular stratigraphic occurrence suggests that anomalously large flows may not only be necessary to mobilize and transport significant amounts of organic matter downslope, but that elevated OM content on the shelf may be partly responsible for triggering such flows and that the frequency of these outsized turbidity currents may be linked to productivity on the outer shelf and over the upper continental slope.

In this model, high rates of organic matter production and fallout would result in the rapid buildup of OM on the seabed that would help to bind and stabilize accumulating sediment (e.g., Bhaskar & Bhosle, 2005; Winterwerp & van Kesteren, 2004; Van Leussen, 2011). These effects then resulted in an overthickening and progressive oversteepening of the sediment pile along the margins of canyons and near the shelf-slope break, which eventually becomes gravitationally unstable resulting in episodic seabed failures that generate large, surge-like flows that are considerably thicker than the depth of the slope channels through which they travel. Accordingly, the flow continuously overspills the channel margins and deposits an anomalously thick, sand- and organic-rich bed. These periodic events not only deplete the shelf of OM, but apparently reduce the slope of the local seabed and result in more typical smaller, organic-poor turbidity currents between these outsized events while the organic-rich sediment pile builds up again. Random, short-lived oceanic events such as upwellings or algal blooms may also have temporarily elevated primary productivity and contributed to the rapid accumulation of organic matter over the outer shelf and upper slope. Thick-bedded, organic-poor sandstone turbidites are interpreted to be less common than thick-bedded, organic-rich sandstone turbidites because without the stabilizing effects of cohesive OM, requisite overthickening and oversteepening of the sediment pile on the shelf and large-scale collapse occur much less frequently, and that these flows initiated from a source located on the OM-impoverished continental slope rather than the continental shelf.

It is also possible that the emplacement of thick, organic-rich turbidites could be related to the formation of large quantities of fluid mud on the shelf. Along modern coasts, particularly near river mouths or estuaries, high primary productivity and OM accumulation aid in the development of fluid mud conditions in the near-bed region by forming large, cohesive, water-saturated aggregates with clay grains (Bachmann et al., 2005; McAnally et al., 2007; Mehta, 1991; Mehta et al., 2014; Otharán et al., 2018). Being unconsolidated and water-saturated, fluid mud is generally easily mobilized (e.g., Anthony et al., 2014; Blanton et al., 1999; McAnally et al., 2007; Otharán et al., 2018; Schrottke et al., 2006; Winterwerp et al., 2017) and in turn has the ability to spawn outsized, organic-rich turbidity currents. However, we consider this interpretation unlikely, since to deposit the organic-rich sandstone beds described here, these fluid mud flows would have to self-ignite (Parker et al., 1986) and incorporate sand as they travelled downslope, as the original suspensions would probably have lacked sufficient sand content.

Significantly, these results suggest that outsized turbidity currents are the primary mechanism for organic matter delivery to the deep sea, and that flow size and frequency, in addition to primary productivity, exerts an important control on the distribution of organic carbon in deep-sea sediments. However, it is important to note that the Windermere turbidite system is Neoproterozoic in age and therefore all the OM was marine and microbial or algal in origin, which then raises the possibility that the conditions described here are unique to deep-sea turbidite systems before the evolution of metazoans or terrestrial plants. Future work could continue to examine Phanerozoic systems to compare how organic matter is sourced and preserved in similar deep-marine settings.

CONCLUSIONS

Observations from well-exposed deep-marine levee deposits of the Neoproterozoic Windermere Supergroup demonstrate that organic matter occurs primarily in thick-bedded, sandstone turbidites with distinct organic-rich and cement-rich bands. These thick, coarse-grained, organic-rich beds are interspersed among more typical organic-poor, thin-bedded levee turbidites and are interpreted to

originate from anomalously thick, continental shelf-derived turbidity currents that continuously overspilled the channel and deposited sediment on the levee. It is proposed that rapid accumulation of organic matter on the continental shelf during periods of high primary productivity contributes to an overthickening and oversteepening of the sediment pile that episodically resulted in outer continental shelf instability and failure and frequent outsized flows. These outsized, continental-shelf- rather than continental-slope-initiated turbidity currents mobilize and transport vast quantities of organic matter and sediment and may be a primary mechanism for organic carbon delivery to deep-marine environments.

Submitted: December 31, 2022 CDT, Accepted: May 11, 2023 CDT

References

Angus, K., Arnott, R. W. C., & Terlaky, V. (2019). Lateral and vertical juxtaposition of matrix-rich and matrix-poor lithologies caused by particle settling in mixed mud-sand deep-marine sediment suspensions. *Sedimentology*, *66*(3), 940–962. https://doi.org/10.1111/sed.12523

Anthony, E. J., Gardel, A., & Gratiot, N. (2014). Fluvial sediment supply, mud banks, cheniers and the morphodynamics of the coast of South America between the Amazon and Orinoco river mouths. *Geological Society, London, Special Publications*, *388*(1), 533–560. https://doi.org/10.1144/sp388.8

Arnott, R. W. C. (2010). Deep-marine sediments and sedimentary systems. In *Facies models* (Vol. 4, pp. 295–322). Geological Association of Canada.

Bachmann, R. W., Hoyer, M. V., Vinzon, S. B., & Canfield, D. Jr. E. (2005). The origin of the fluid mud layer in Lake Apopka, Florida. *Limnology and Oceanography*, *50*(2), 629–635. https://doi.org/10.4319/lo.2005.50.2.0629

Baudin, F., Disnar, J.-R., Martinez, P., & Dennielou, B. (2010). Distribution of the organic matter in the channel-levees systems of the Congo mud-rich deep-sea fan (West Africa). Implication for deep offshore petroleum source rocks and global carbon cycle. *Marine and Petroleum Geology*, *27*(5), 995–1010. https://doi.org/10.1016/j.marpetgeo.2010.02.006

Baudin, F., Rabouille, C., & Dennielou, B. (2020). Routing of terrestrial organic matter from the Congo River to the ultimate sink in the abyss: a mass balance approach (André Dumont medallist lecture 2017). *Geologica Belgica*, *23*(1–2). https://doi.org/10.20341/gb.2020.004

Baudin, F., Stetten, E., Schnyder, J., Charlier, K., Martinez, P., Dennielou, B., & Droz, L. (2017). Origin and distribution of the organic matter in the distal lobe of the Congo deep-sea fan – A Rock-Eval survey. *Deep Sea Research Part II: Topical Studies in Oceanography*, *142*, 75–90. https://doi.org/10.1016/j.dsr2.2017.01.008

Behrensmeyer, A. K., Damuth, J. D., DiMichele, W. A., Potts, R., Sues, H. D., & Wings, S. L. (1992). *Terrestrial ecosystems through time. evolutionary paleoecology of terrestrial plants and animals*. University of Chicago Press.

Bergen, A. L., Cunningham, C. M., Terlaky, V., & Arnott, R. W. C. (2022). Influence of channelized-flow density structure on the stratal architecture of deep-marine levee deposits. *Journal of Sedimentary Research*, *92*(4), 381–403. https://doi.org/10.2110/jsr.2020.183

Bhaskar, P. V., & Bhosle, N. B. (2005). Microbial extracellular polymeric substances in marine biogeochemical processes. *Current Science*, *v. 88*, 45–53.

Blanton, J., Alexander, C., Alber, M., & Kineke, G. (1999). The mobilization and deposition of mud deposits in a coastal plain estuary. *Limnologica*, *29*(3), 293–300. https://doi.org/10.1016/s0075-9511(99)80016-4

Boles, J. R. (1978). Active ankerite cementation in the subsurface Eocene of Southwest Texas. *Contributions to Mineralogy and Petrology*, *68*(1), 13–22. https://doi.org/10.1007/bf00375443

Bornhold, B. D., Ren, P., & Prior, D. B. (1994). High-frequency turbidity currents in British Columbia fjords. *Geo-Marine Letters*, *14*(4), 238–243. https://doi.org/10.1007/bf01274059

Bouma, A. H. (1962). *Sedimentology of some Flysch deposits: a graphic approach to facies interpretation: Amsterdam*. Elsevier.

Butterfield, N. J. (2014). Early evolution of the Eukaryota. *Palaeontology*, *58*(1), 5–17. https://doi.org/10.1111/pala.12139

Campbell, R. B., Mountjoy, E. W., & Young, F. G. (1973). *Geology of McBride map-area, British Columbia (93H)* (Geological Survey of Canada, Paper 72–35, p. 104). Natural Resources Canada/CMSS/Information Management. https://doi.org/10.4095/103468

Colpron, M., Logan, J. M., & Mortensen, J. K. (2002). U-Pb zircon age constraint for late Neoproterozoic rifting and initiation of the lower Paleozoic passive margin of western Laurentia. *Canadian Journal of Earth Sciences*, *39*(2), 133–143. https://doi.org/10.1139/e01-069

Cunningham, C. M., & Arnott, R. W. C. (2021). Systematic organization of thin-bedded turbidites in ancient deep-marine levees: Possible evidence of rhythmic pulsing in turbidity currents. *Journal of Sedimentary Research*, *91*(11), 1257–1274. https://doi.org/10.2110/jsr.2021.003

Cunningham, C. M., & Arnott, R. W. C. (2023). Organic matter deposition and preservation in ancient deep-sea levee sediments: Implications for global trends in carbon burial. *Sedimentology*, *70*(2), 475–504. https://doi.org/10.1111/sed.13052

Cunningham, C. M., Ruso, S. F., & Arnott, R. W. C. (2023). Controls on the stratigraphic distribution of organic carbon in ancient deep-marine levees. *Marine and Petroleum Geology*, *148*, 106039. https://doi.org/10.1016/j.marpetgeo.2022.106039

Curtis, C. D. (1978). Possible links between sandstone diagenesis and depth-related geochemical reactions occurring in enclosing mudstones. *Journal of the Geological Society*, *135*(1), 107–117. https://doi.org/10.1144/gsjgs.135.1.0107

Evenchick, C. A., Parrish, R. R., & Gabrielse, H. (1984). Precambrian gneiss and late Proterozoic sedimentation in north-central British Columbia. *Geology*, *12*(4), 233. https://doi.org/10.1130/0091-7613(1984)12

Eyster, A., Ferri, F., Schmitz, M. D., & Macdonald, F. A. (2018). One diamictite and two rifts: Stratigraphy and geochronology of the Gataga Mountain of northern British Columbia. *American Journal of Science*, *318*(2), 167–207. https://doi.org/10.2475/02.2018.1

Galy, V., France-Lanord, C., Beyssac, O., Faure, P., Kudrass, H., & Palhol, F. (2007). Efficient organic carbon burial in the Bengal fan sustained by the Himalayan erosional system. *Nature*, *450*(7168), 407–410. https://doi.org/10.1038/nature06273

Gensel, P. G. (2021). When did terrestrial plants arise? *Science*, *373*(6556), 736–737. https://doi.org/10.1126/science.abl5297

Hadlari, T., Arnott, R. W. C., Matthews, W. A., Poulton, T. P., Root, K., & Madronich, L. I. (2021). Provenance of the Incipient Passive Margin of NW Laurentia (Neoproterozoic): Detrital Zircon from Continental Slope and Basin Floor Deposits of the Windermere Supergroup, Southern Canadian Cordillera. *Lithosphere*, *2021*(1), 10. https://doi.org/10.2113/2021/8356327

Hage, S., Cartigny, M. J. B., Sumner, E. J., Clare, M. A., Hughes Clarke, J. E., Talling, P. J., Lintern, D. G., Simmons, S. M., Silva Jacinto, R., Vellinga, A. J., Allin, J. R., Azpiroz-Zabala, M., Gales, J. A., Hizzett, J. L., Hunt, J. E., Mozzato, A., Parsons, D. R., Pope, E. L., Stacey, C. D., … Watts, C. (2019). Direct monitoring reveals initiation of turbidity currents from extremely dilute river plumes. *Geophysical Research Letters*, *46*(20), 11310–11320. https://doi.org/10.1029/2019gl084526

Hage, S., Galy, V., Cartigny, M. J. B., Heerema, C., Heijnen, M. S., Acikalin, S., Clare, M. A., Giesbrecht, I. J. W., Gröcke, D. R., Hendry, A., Hilton, R. G., Hubbard, S. M., Hunt, J. E., Lintern, G., McGhee, C., Parsons, D. R., Pope, E. L., Stacey, C. D., Sumner, E. J., … Talling, P. (2022). Turbidity currents can dictate organic carbon fluxes across river-fed fjords: An example from Bute Inlet (BC, Canada). *Journal of Geophysical Research: Biogeosciences*, 2022006824. https://doi.org/10.1002/essoar.10510464.2

Hage, S., Galy, V. V., Cartigny, M. J. B., Acikalin, S., Clare, M. A., Gröcke, D. R., Hilton, R. G., Hunt, J. E., Lintern, D. G., McGhee, C. A., Parsons, D. R., Stacey, C. D., Sumner, E. J., & Talling, P. J. (2020). Efficient preservation of young terrestrial organic carbon in sandy turbidity-current deposits. *Geology*, *48*(9), 882–887. https://doi.org/10.1130/g47320.1

Hayes, J. M., Kaplan, I. R., & Wedeking, K. W. (1983). Precambrian organic geochemistry, preservation of the record. In J. W. Schopf (Ed.), *Earth's Earliest Biosphere: Its Origin and Evolution* (pp. 93–134). Princeton University Press.

Hsu, S.-K., Kuo, J., Lo, C.-L., Tsai, C.-H., Doo, W.-B., Ku, C.-Y., & Sibuet, J.-C. (2008). Turbidity currents, submarine landslides and the 2006 Pingtung earthquake off SW Taiwan. *Terrestrial, Atmospheric and Oceanic Sciences*, *19*(6), 767. https://doi.org/10.3319/tao.2008.19.6.767(pt)

Hussain, A., Haughton, P. D. W., Shannon, P. M., Morris, E. A., Pierce, C. S., & Omma, J. E. (2021). Mud-forced turbulence dampening facilitates rapid burial and enhanced preservation of terrestrial organic matter in deep-sea environments. *Marine and Petroleum Geology*, *130*, 105101. https://doi.org/10.1016/j.marpetgeo.2021.105101

Kane, I. A., Kneller, B. C., Dykstra, M., Kassem, A., & McCaffrey, W. D. (2007). Anatomy of a submarine channel–levee: An example from Upper Cretaceous slope sediments, Rosario Formation, Baja California, Mexico. *Marine and Petroleum Geology*, *24*(6–9), 540–563. https://doi.org/10.1016/j.marpetgeo.2007.01.003

Kelts, K., & McKenzie, J. (1982). Diagenetic dolomite formation in Quaternary anoxic diatomaceous muds of Deep Sea Drilling Project Leg 64, Gulf of California. In J. R. Curray … D. G. Moore, *Initial reports of the Deep Sea Drilling Project* (Vol. 64, pp. 553–569). U.S. Government Printing Office.

Kendall, B. S., Creaser, R. A., Ross, G. M., & Selby, D. (2004). Constraints on the timing of Marinoan "Snowball Earth" glaciation by 187Re–187Os dating of a Neoproterozoic, post-glacial black shale in Western Canada. *Earth and Planetary Science Letters*, *222*(3–4), 729–740. https://doi.org/10.1016/j.epsl.2004.04.004

Khan, Z. (2012). *Origin and architecture of deep-water level deposits: Insight from the ancient rock record and experiments* [Unpublished Ph.D. thesis,]. University of Ottawa.

Khan, Z. A., Arnott, B., & Pugin, A. (2011). An alternative model of producing topography in the crest region of deep-water levees. *American Association of Petroleum Geologists Bulletin*, *95*(12), 2085–2106. https://doi.org/10.1306/03281110024

Khan, Z. A., & Arnott, R. W. C. (2011). Stratal attributes and evolution of asymmetric inner- and outer-bend levee deposits associated with an ancient deep-water channel-levee complex within the Isaac Formation, southern Canada. *Marine and Petroleum Geology*, *28*(3), 824–842. https://doi.org/10.1016/j.marpetgeo.2010.07.009

Krause, D. C., White, W. C., Piper, D. J. W., & Heezen, B. C. (1970). Turbidity currents and cable breaks in the western New Britain Trench. *Geological Society of America Bulletin*, *81*(7), 2153. https://doi.org/10.1130/0016-7606(1970)81

Lee, H., Galy, V., Feng, X., Ponton, C., Galy, A., France-Lanord, C., & Feakins, S. J. (2019). Sustained wood burial in the Bengal Fan over the last 19 My. *Proceedings of the National Academy of Sciences*, *116*(45), 22518–22525. https://doi.org/10.1073/pnas.1913714116

Leussen, W. (2011). Macroflocs, fine-grained sediment transports, and their longitudinal variations in the Ems Estuary. *Ocean Dynamics*, *61*(2–3), 387–401. https://doi.org/10.1007/s10236-011-0384-9

Lund, K., Aleinikoff, J. N., Evans, K. V., & Fanning, C. M. (2003). SHRIMP U-Pb geochronology of Neoproterozoic Windermere Supergroup, central Idaho: Implications for rifting of western Laurentia and synchroneity of Sturtian glacial deposits. *Geological Society of America Bulletin*, *115*, 349–372. https://doi.org/10.1130/0016-7606(2003)115

Masiello, C. A. (2007). Quick burial at sea. *Nature*, *450*(7168), 360–361. https://doi.org/10.1038/450360a

Masson, D. G., Arzola, R. G., Wynn, R. B., Hunt, J. E., & Weaver, P. P. E. (2011). Seismic triggering of landslides and turbidity currents offshore Portugal. *Geochemistry, Geophysics, Geosystems*, *12*(12). https://doi.org/10.1029/2011gc003839

Mazzullo, S. J. (2000). Organogenic dolomitization in peritidal to deep-sea sediments. *Journal of Sedimentary Research*, *70*(1), 10–23. https://doi.org/10.1306/2dc408f9-0e47-11d7-8643000102c1865d

McAnally, W. H., Friedrichs, C., Hamilton, D., Hayter, E., Shrestha, P., Rodriguez, H., Sheremet, A., Teeter, A., & ASCE Task Committee on Management of Fluid Mud. (2007). Management of fluid mud in estuaries, bays, and lakes. I: Present state of understanding on character and behavior. *Journal of Hydraulic Engineering*, *133*(1), 9–22. https://doi.org/10.1061/(asce)0733-9429(2007)133:1(9)

McArthur, A. D., Gamberi, F., Kneller, B. C., Wakefield, M. I., Souza, P. A., & Kuchle, J. (2017). Palynofacies classification of submarine fan depositional environments: Outcrop examples from the Marnoso-Arenacea Formation, Italy. *Marine and Petroleum Geology*, *88*, 181–199. https://doi.org/10.1016/j.marpetgeo.2017.08.018

McArthur, A. D., Kneller, B. C., Souza, P. A., & Kuchle, J. (2016). Characterization of deep-marine channel-levee complex architecture with palynofacies: An outcrop example from the Rosario Formation, Baja California, Mexico. *Marine and Petroleum Geology*, *73*, 157–173. https://doi.org/10.1016/j.marpetgeo.2016.02.030

McArthur, A. D., Kneller, B. C., Wakefield, M. I., Souza, P. A., & Kuchle, J. (2016). Palynofacies classification of the depositional elements of confined turbidite systems: Examples from the Gres d'Annot, SE France. *Marine and Petroleum Geology*, *77*, 1254–1273. https://doi.org/10.1016/j.marpetgeo.2016.08.020

McDonough, M. R., & Parrish, R. R. (1991). Proterozoic gneisses of the Malton Complex, near Valemount, British Columbia: U–Pb ages and Nd isotopic signatures. *Canadian Journal of Earth Sciences*, *28*(8), 1202–1216. https://doi.org/10.1139/e91-108

Mehta, A. J. (1991). Understanding fluid mud in a dynamic environment. *Geo-Marine Letters*, *11*(3–4), 113–118. https://doi.org/10.1007/bf02430995

Mehta, A. J., Samsami, F., Khare, Y. P., & Sahin, C. (2014). Fluid mud properties in nautical depth estimation. *Journal of Waterway, Port, Coastal, and Ocean Engineering*, *140*(2), 210–222. https://doi.org/10.1061/(asce)ww.1943-5460.0000228

Mountjoy, J. J., Howarth, J. D., Orpin, A. R., Barnes, P. M., Bowden, D. A., Rowden, A. A., Schimel, A. C. G., Holden, C., Horgan, H. J., Nodder, S. D., Patton, J. R., Lamarche, G., Gerstenberger, M., Micallef, A., Pallentin, A., & Kane, T. (2018). Earthquakes drive large-scale submarine canyon development and sediment supply to deep-ocean basins. *Science Advances*, *4*(3), 3748. https://doi.org/10.1126/sciadv.aar3748

Navarro, L., & Arnott, R. W. C. (2020). Stratigraphic record in the transition from basin floor to continental slope sedimentation in the ancient passive-margin Windermere turbidite system. *Sedimentology*, *67*(4), 1710–1749. https://doi.org/10.1111/sed.12676

Ningthoujam, J., Wearmouth, C., & Arnott, R. W. C. (2022). Stratal characteristic and depositional origin of two-part (Mud-poor overlain by mud-rich) and associated deep-water strata: Components in a lateral depositional continuum related to particle settling in negligibly sheared mud-rich suspensions. *Journal of Sedimentary Research*, *92*(6), 503–529. https://doi.org/10.2110/jsr.2021.053

Normandeau, A., Bourgault, D., Neumeier, U., Lajeunesse, P., St-Onge, G., Gostiaux, L., & Chavanne, C. (2020). Storm-induced turbidity currents on a sediment-starved shelf: Insight from direct monitoring and repeat seabed mapping of upslope migrating bedforms. *Sedimentology*, *67*(2), 1045–1068. https://doi.org/10.1111/sed.12673

Otharán, G. A., Zavala, C., Arcuri, M., Marchal, D., Köhler, G., Di Meglio, M., & Zorzano, A. (2018). The role of fluid mud flows in the accumulation of organic-rich shales. *The Upper Jurassic-Lower Cretaceous Vaca Muerta Formation, Neuquén Basin, Argentina. In Simposio de Recursos No Convencionales. Mendoza, Proceedings*, 61–90.

Parker, G., Fukushima, Y., & Pantin, H. M. (1986). Self-accelerating turbidity currents. *Journal of Fluid Mechanics*, *171*(1), 145. https://doi.org/10.1017/s0022112086001404

Peakall, J., McCaffrey, W. D., & Kneller, B. C. (2000). A process model for the evolution, morphology, and architecture of sinuous submarine channels. *Journal of Sedimentary Research*, *70*(3), 434–448. https://doi.org/10.1306/2dc4091c-0e47-11d7-8643000102c1865d

Piper, D. J. W., & Normark, W. R. (2009). Processes That Initiate Turbidity Currents and Their Influence on Turbidites: A Marine Geology Perspective. *Journal of Sedimentary Research*, *79*(6), 347–362. https://doi.org/10.2110/jsr.2009.046

Porcile, G., Bolla Pittaluga, M., Frascati, A., & Sequeiros, O. E. (2020). Typhoon-induced megarips as triggers of turbidity currents offshore tropical river deltas. *Communications Earth & Environment*, *1*(1), 1–13. https://doi.org/10.1038/s43247-020-0002-1

Ross, G. M. (1991). Tectonic setting of the Windermere Supergroup revisited. *Geology*, *v. 19*, 1125–1128. https://doi.org/10.1130/00917613(1991)019<1125:TSOTWS>2.3.CO;2

Ross, G. M., & Arnott, R. W. C. (2007). Regional geology of the Windermere Supergroup, southern Canadian Cordillera and stratigraphic setting of the Castle Creek study area, Canada. In T. H. Nilsen, R. D. Shew, & J. R. J. Studlick (Eds.), *Atlas of Deep-water Outcrops. American Association of Petroleum Geologists, Studies in Geology: Vol. v. 56* (p. 22).

Ross, G. M., Bloch, J. D., & Krouse, H. R. (1995). Neoproterozoic strata of the southern Canadian Cordillera and the isotopic evolution of seawater sulfate. *Precambrian Research*, *73*(1–4), 71–99. https://doi.org/10.1016/0301-9268(94)00072-y

Russell, A. J., Roberts, M. J., Fay, H., Marren, P. M., Cassidy, N. J., Tweed, F. S., & Harris, T. (2006). Icelandic jökulhlaup impacts: implications for ice-sheet hydrology, sediment transfer and geomorphology. *Geomorphology*, *75*(1–2), 33–64. https://doi.org/10.1016/j.geomorph.2005.05.018

Saller, A., Lin, R., & Dunham, J. (2006). Leaves in turbidite sands: The main source of oil and gas in the deep-water Kutei Basin, Indonesia. *American Association of Petroleum Geologists Bulletin*, *90*(10), 1585–1608. https://doi.org/10.1306/04110605127

Schrottke, K., Becker, M., Bartholomä, A., Flemming, B. W., & Hebbeln, D. (2006). Fluid mud dynamics in the Weser estuary turbidity zone tracked by high-resolution side-scan sonar and parametric sub-bottom profiler. *Geo-Marine Letters*, *26*(3), 185–198. https://doi.org/10.1007/s00367-006-0027-1

Sequeiros, O. E., Bolla Pittaluga, M., Frascati, A., Pirmez, C., Masson, D. G., Weaver, P., Crosby, A. R., Lazzaro, G., Botter, G., & Rimmer, J. G. (2019). How typhoons trigger turbidity currents in submarine canyons. *Scientific Reports*, *9*(1), 1–15. https://doi.org/10.1038/s41598-019-45615-z

Shaw, J., & Gilbert, R. (1990). Evidence for large-scale subglacial meltwater flood events in southern Ontario and northern New York State. *Geology*, *18*(12), 1169. https://doi.org/10.1130/0091-7613(1990)018

Smith, M. D., Arnott, R. W. C., & Ross, G. M. (2014). Physical and geochemical controls on sedimentation along an ancient continental margin: The deep-marine Old Fort Point Formation (Ediacaran), southern Canadian Cordillera. *Bulletin of Canadian Petroleum Geology*, *62*(1), 14–36. https://doi.org/10.2113/gscpgbull.62.1.14

Stetten, E., Baudin, F., Reyss, J.-L., Martinez, P., Charlier, K., Schnyder, J., Rabouille, C., Dennielou, B., Coston-Guarini, J., & Pruski, A. M. (2015). Organic matter characterization and distribution in sediments of the terminal lobes of the Congo deep-sea fan: evidence for the direct influence of the Congo River. *Marine Geology*, *369*, 182–195. https://doi.org/10.1016/j.margeo.2015.08.020

Talling, P. J. (2014). On the triggers, resulting flow types and frequencies of subaqueous sediment density flows in different settings. *Marine Geology*, *352*, 155–182. https://doi.org/10.1016/j.margeo.2014.02.006

Talling, P. J., Baker, M. L., Pope, E. L., Ruffell, S. C., Jacinto, R. S., Heijnen, M. S., Hage, S., Simmons, S. M., Hasenhündl, M., Heerema, C. J., McGhee, C., Apprioual, R., Ferrant, A., Cartigny, M. J. B., Parsons, D. R., Clare, M. A., Tshimanga, R. M., Trigg, M. A., Cula, C. A., ... Hilton, R. J. (2022). Longest sediment flows yet measured show how major rivers connect efficiently to deep sea. *Nature Communications*, *13*(1), 4193. https://doi.org/10.1038/s41467-022-31689-3

Terlaky, V., & Arnott, R. W. C. (2014). Matrix-rich and associated matrix-poor sandstones: avulsion splays in slope and basin-floor strata. *Sedimentology*, *61*, 1175–1197. https://doi.org/10.1111/sed.12096

Terlaky, V., Rocheleau, J., & Arnott, R. W. C. (2015). Stratal composition and stratigraphic organization of stratal elements in an ancient deep-marine basin-floor succession, Neoproterozoic Windermere Supergroup, British Columbia, Canada. *Sedimentology*, *63*(1), 136–175. https://doi.org/10.1111/sed.12222

Tissot, B. P., & Welte, D. H. (1978). Sedimentary processes and the accumulation of organic matter. In B.P. Tissot & D. H. Welte (Eds.), *Petroleum Formation and Occurrence: A New Approach to Oil and Gas Exploration* (pp. 55–62). Springer-verlag. https://doi.org/10.1007/978-3-642-96446-6_5

Tweed, F. S., & Russell, A. J. (1999). Controls on the formation and sudden drainage of glacier-impounded lakes: implications for jökulhlaup characteristics. *Progress in Physical Geography: Earth and Environment*, *23*(1), 79–110. https://doi.org/10.1177/030913339902300104

Veh, G., Korup, O., von Specht, S., Roessner, S., & Walz, A. (2019). Unchanged frequency of moraine-dammed glacial lake outburst floods in the Himalaya. *Nature Climate Change*, *9*(5), 379–383. https://doi.org/10.1038/s41558-019-0437-5

Weckwerth, P., Wysota, W., Piotrowski, J. A., Adamczyk, A., Krawiec, A., & Dąbrowski, M. (2019). Late Weichselian glacier outburst floods in North-Eastern Poland: Landform evidence and palaeohydraulic significance. *Earth-Science Reviews*, *194*, 216–233. https://doi.org/10.1016/j.earscirev.2019.05.006

Winterwerp, J. C., & van Kesteren, W. G. M. (2004). *Introduction to the Physics of Cohesive Sediment Dynamics in the Marine Environment*. Elsevier.

Winterwerp, J. C., Vroom, J., Wang, Z.-B., Krebs, M., Hendriks, E. C. M., van Maren, D. S., Schrottke, K., Borgsmüller, C., & Schöl, A. (2017). SPM response to tide and river flow in the hyper-turbid Ems River. *Ocean Dynamics*, *67*(5), 559–583. https://doi.org/10.1007/s10236-017-1043-6

Zhang, Y., Liu, Z., Zhao, Y., Colin, C., Zhang, X., Wang, M., Zhao, S., & Kneller, B. (2018). Long-term in situ observations on typhoon-triggered turbidity currents in the deep sea. *Geology*, *46*(8), 675–678. https://doi.org/10.1130/g45178.1